Cell

The Conserved microRNA MiR-8 Tunes Atrophin Levels to Prevent Neurodegeneration in Drosophila

Janina S. Karres,[1] Valérie Hilgers,[1] Ines Carrera,[3] Jessica Treisman,[3] and Stephen M. Cohen[1,2,*]
[1]European Molecular Biology Laboratory, Meyerhofstrasse 1, 69117 Heidelberg, Germany
[2]Temasek Life Sciences Laboratory, and Department of Biological Sciences, National University of Singapore, 1 Research Link, Singapore 117604
[3]Skirball Institute, New York University, 540 First Avenue, New York, NY 10016, USA
*Correspondence: cohen@tll.org.sg
DOI 10.1016/j.cell.2007.09.020

SUMMARY

microRNAs (miRNAs) bind to specific messenger RNA targets to posttranscriptionally modulate their expression. Understanding the regulatory relationships between miRNAs and targets remains a major challenge. Many miRNAs reduce expression of their targets to inconsequential levels. It has also been proposed that miRNAs might adjust target expression to an optimal level. Here we analyze the consequences of mutating the conserved miRNA *miR-8* in *Drosophila*. We identify *atrophin* as a direct target of miR-8. *miR-8* mutant phenotypes are attributable to elevated *atrophin* activity, resulting in elevated apoptosis in the brain and in behavioral defects. Reduction of atrophin levels in miR-8-expressing cells to below the level generated by miR-8 regulation is detrimental, providing evidence for a "tuning target" relationship between them. *Drosophila atrophin* is related to the atrophin family of mammalian transcriptional regulators, implicated in the neurodegenerative disorder DRPLA. The regulatory relationship between miR-8 and atrophin orthologs is conserved in mammals.

INTRODUCTION

microRNAs (miRNAs) are short noncoding RNAs that serve as posttranscriptional regulators of gene expression in plants and animals (reviewed in Kloosterman and Plasterk, 2006; Mallory and Vaucheret, 2006; Bushati and Cohen, 2007). The roles of miRNAs in animal development have been the subject of considerable interest. Hundreds of miRNAs have been identified, and computational methods have predicted hundreds of targets for the average miRNA, leading to proposals that one-third or more of the transcriptome may be miRNA regulated (e.g., Brennecke et al., 2005; Grun et al., 2005; Lewis et al., 2005; Stark et al., 2005).

Recent studies comparing miRNA and target expression have suggested that many miRNAs serve to limit target gene expression in tissues, where target expression is normally low and where leaky expression would be detrimental (Farh et al., 2005; Stark et al., 2005). Acting in this mode, miRNAs can be thought of as having a switch-like function to eliminate target expression (Bartel and Chen, 2004). The idea of mutual exclusion can also operate temporally. An elegant example of this is the role of miR-430, the first miRNA expressed in the zebrafish embryo, in promoting turnover of maternally encoded mRNAs (Giraldez et al., 2005). These studies have led to the proposal that the main role of many miRNAs is to exclude target RNA expression to ensure robustness of developmental processes (Stark et al., 2005; Hornstein and Shomron, 2006). A recent study of the miR-9b miRNA mutant has shown a phenotype best described as a failure in robustness (Li et al., 2006). miR-9b sets a threshold for activation of a positive feedback loop involved in cell-fate specification in sensory nervous system of *Drosophila* by regulating the proneural transcription factor senseless (Nolo et al., 2000). Failure to limit senseless expression leads to a sporadic activation and to variability in the number of sensory organs produced.

Another possible mode of miRNA function involves "tuning" the expression level of target RNAs with which they are normally coexpressed (Bartel and Chen, 2004). Although this model is appealing, it has received little experimental support to date from study of miRNA functions in vivo. Here, we analyze the functions of *miR-8* in *Drosophila* and identify the transcriptional regulator atrophin as a direct functional target of this miRNA. Atrophin is broadly expressed during development, and defects associated with *miR-8* mutants are attributable to a failure to limit atrophin expression in *miR-8*-expressing cells, resulting in elevated apoptosis in the brain and behavioral defects. We provide evidence that miR-8 tunes the level of atrophin expression, because further reduction of

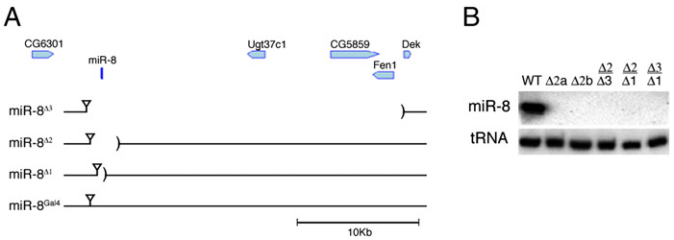

Figure 1. MiR-8 Mutants

(A) Schematic representation of the *miR-8* locus. *miR-8* is located on chromosome 2R at 53D11 on the cytological map. Lower panel: breakpoints of three *miR-8* mutant alleles and the insertion sites of the P elements used to generate these alleles. The insertion site of the Gal4 containing P element (*miR-8*^{Gal4}) is indicated. *miR-8*$^{\Delta 3}$ was generated by male recombination using the P element EP2239. The deletion spans 26 kb, and the breakpoint was determined by DNA sequencing. *miR-8*$^{\Delta 2}$ was produced via imprecise excision by mobilization of P element EP2269, and the deletion spans 1.8 kb. *miR-8*$^{\Delta 1}$ was produced by targeted knockout. Four hundred base pairs spanning the miR-8 locus was replaced by the miniwhite gene.

(B) Northern blot showing miR-8 RNA in a wild-type control and *miR-8* mutant allelic combinations. Δ2a and Δ2b are independent homozygous lines of *miR-8*$^{\Delta 2}$.

atrophin levels in miR-8-expressing cells is detrimental. Regulation of atrophin by miR-8 constitutes a biologically significant example of tuning target mRNA expression in the nervous system. Further, this study implicates miR-8 in development and function of the nervous system and suggests a possible connection to neurodegenerative disease.

RESULTS

miR-8 Mutants

To analyze the function of *miR-8* in *Drosophila* we generated loss of function mutant alleles (Figure 1A). *mir-8*$^{\Delta 1}$ was produced by homologous recombination. A 400 bp fragment, spanning the miR-8 hairpin, was replaced by the miniwhite gene. *miR-8*$^{\Delta 2}$ and *miR-8*$^{\Delta 3}$ were produced by imprecise excision of the *P* elements *P*(EP)2269 and *P*(EP)2239. The deletions removed 1.8 kb and 26 kb, respectively. Northern blot analysis confirmed that the mature miR-8 product was not produced in any of the three alleles (Figure 1B).

The phenotypes resulting from removal of *miR-8* were analyzed in the three possible allelic combinations to exclude potential effects of genetic background. Although *miR-8* is expressed in a complex pattern in the embryo and in larvae (Figure S1), mutants lacking *miR-8* completed larval development normally but showed reduced survival during pupal and early adult stages (Figure 2A). Of the 14%–19% of mutants that died, ~80% failed to emerge from the pupal case and the remainder died within the first 24 hr of adult life. Most of this latter group had malformed third legs. Thirty-three to fifty percent of the surviving adults showed a similar leg defect (Figures 2C and 2E). Twenty-two to thirty-two percent of the surviving adults had wings that were not properly unfolded (Figures 2B and 2D). In this analysis, mutant animals were separated from their heterozygous siblings to minimize the effects of competition with healthier animals during larval stages. Survival of the mutants was reduced further when they were reared together with their siblings (e.g., Figure 5B).

To examine the basis for these morphological defects, we performed a genetic mosaic analysis. Clones of *miR-8* mutant cells produced in the leg and wing imaginal discs did not cause morphological defects in adult wings or legs. This suggests that the observed defects were not due to a requirement for *miR-8* activity in the imaginal disc epithelia per se, although *miR-8* is expressed there (Figures S1F and S1G). Although malformed, *miR-8* mutant legs and wings were patterned normally. Such defects might result from improper unfolding of the imaginal discs during emergence of the adult fly from the pupal case. Time-lapse imaging showed that wild-type flies freed themselves from the pupal case very rapidly. *miR-8* mutants, in contrast, appeared to have difficulty detaching themselves, with a leg or wing often becoming entangled (Movie S1). Many mutants died after several hours of struggle. Mechanical damage to legs and wings can occur in those that manage to pull free, particularly if they fail to do so before the adult cuticle hardens. The leg abnormalities may also reflect an earlier defect. Leg and wing imaginal disc morphogenesis involves eversion of the disc epithelium and elongation during pupal stages (see Fristrom and Fristrom, 1993). *miR-8* mutants often failed to extend their legs properly within the pupal case and showed mild malformations (Figure S2). It has been suggested that pressure generated by contraction of the abdominal muscles is a major driving force for leg and wing extension at the prepupal-pupal transition (Fortier et al., 2003). Impaired neuromuscular coordination could cause the defects we observed in *miR-8* mutant legs.

MiR-8 Regulates Atrophin

miRNAs are predicted to have many targets (Brennecke et al., 2005; Lewis et al., 2005; Grun et al., 2005; Xie et al., 2005; Krek et al., 2005). *Drosophila* miR-8 has over 250 conserved predicted targets (Stark et al., 2005; Grun et al., 2005). In view of its complex spatial and temporal expression pattern (Figure S1), miR-8 might be expected to regulate different target RNAs in different contexts. Misregulation of only a small subset of these might be responsible for the observed mutant phenotypes. Previous reports have shown that target RNA levels can be altered either by overexpressing miRNAs in cells where they are not normally expressed (Lim et al., 2005; Behm-Ansmant et al., 2006), by eliminating miRNA production globally (Giraldez et al., 2006; Rehwinkel et al., 2006) or using mutants that remove specific miRNAs

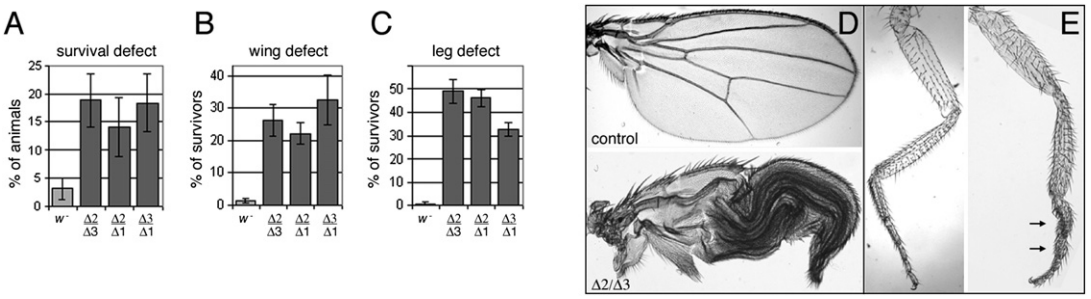

Figure 2. MiR-8 Mutant Phenotypes

(A–C) Histograms illustrating the severity of the defects in the three different *miR-8* mutant combinations. Animals were grown under controlled conditions. The data represent an average ± standard deviation (SD) of 8 batches of 100 flies for each genotype. (A) shows the reduced survival of adult flies. Approximately 80% of the dead individuals failed to eclose from the pupal case. The remainder died within the first 24 hr after eclosion. Most of these animals had a malformed third leg. (B) shows the percentage of surviving adults with wing defects. Wings of *miR-8* mutants often failed to unfold normally (see D). (C) shows the percentage of surviving adults with leg defects. The third leg pairs of *miR-8* mutant animals were often severely malformed (see E). (D) and (E) show cuticle preparations of control and *miR-8* mutant wings and legs.

(Teleman et al., 2006). In this context, we looked for genes predicted to be miR-8 targets that were upregulated in *miR-8* mutants. Expression profiling was performed using two combinations of *miR-8* mutant alleles. RNA was prepared from pupae, as the *mir-8* mutant phenotypes were apparent during late pupal stages. Approximately 200 genes were reproducibly upregulated by at least 2-fold in *miR-8* mutants (Table S1). This group is expected to include direct miR-8 targets and genes affected indirectly. The latter group likely predominates, as a similar number of RNAs were downregulated. Among the upregulated genes, only four had miR-8 target sites that were conserved between *D. melanogaster* and D. pseudoobscura: CG13060, CG8420, CG9036, and CG6964 (*Drosophila atrophin*).

miRNA target sites are most often found in 3′UTRs. The *atrophin* 3′UTR has four potential miR-8 target sites, two of which are conserved in D. pseudoobscura (Figure 3A). Interestingly, this regulatory relationship appears to be conserved in mammals. Two human miRNAs, miR-200b and miR-429, are identical to miR-8 in the seed region (residues 2–8), the major determinant of miRNA target specificity (Brennecke et al., 2005; Lewis et al., 2005). Three potential target sites for miR-200b and miR-429 were found in the 3′UTR of the human othologue of atrophin, RERE (Figure 3B).

On the basis of the apparent conservation of this regulatory relationship, we focused our analysis on *atrophin* as a possible miR-8 target. We first verified the microarray results by quantitative real-time RT-PCR. *atrophin* mRNA levels were ~2-fold higher in homozygous *miR-8* mutants at early pupal stages (Figure 4A). In view of the change in *atrophin* mRNA level, it was of interest to determine whether the effect of miR-8 was directly posttranscriptional or indirect, reflecting a change in transcription. To address this, we performed real-time RT-PCR comparing the level of the nuclear *atrophin* primary transcript with that of the mature mRNA. miRNA-mediated gene regulation takes place in the cytoplasm and so should not affect the primary transcript in the nucleus. Real-time RT-PCR using intron-specific primers provides a means to compare *atrophin* primary transcript levels with the levels of the mature mRNA in the cytoplasm, using primers located in the exons. If upregulation of *atrophin* mRNA was due to increased transcription, we would expect primary transcript levels to increase in *miR-8* mutants. However, this proved not to be the case. Only the mature mRNA level increased (Figure 4A). Thus, the increase in *atrophin* mRNA in the *miR-8* mutant is posttranscriptional, suggesting that miR-8 binding leads to destabilization of *atrophin* mRNA.

Can the effect on *atrophin* mRNA stability be attributed to the miR-8 sites in its 3′UTR? To address this, we generated transgenic flies expressing a *luciferase* reporter gene linked to the *atrophin* 3′UTR or a version of this UTR in which the miR-8 sites were mutated. Q-PCR analysis showed that the level of *luciferase* mRNA increased in the *miR-8* mutants for the construct with the intact miR-8 sites, but not when these sites were mutated (Figure 4B). Coexpression of the luciferase reporters in S2 cells with miR-8 reduced *luciferase* mRNA levels to ~60% (Figure 4C). A comparable reduction of luciferase enzyme activity was observed in response to miR-8 (Figure 4D), and this effect was largely eliminated when the miR-8 sites were mutated (Figure 4D). Together these observations provide evidence that miR-8 acts directly via these sites to control *atrophin* expression in vivo. miR-429 and miR-200b were also able to regulate a luciferase reporter containing the human RERE 3′UTR (Figures 4E and 4F), suggesting conservation of this relationship.

Atrophin Overexpression Contributes to the *miR-8* Mutant Phenotype

To ask whether atrophin protein levels were elevated in the *miR-8* mutants, we performed immunoblots on lysates from control flies and two *miR-8* mutant combinations. As a positive control for antibody specificity we used flies overexpressing the endogenous *atrophin* gene from an EP element insertion under Gal4 control. Lysates were

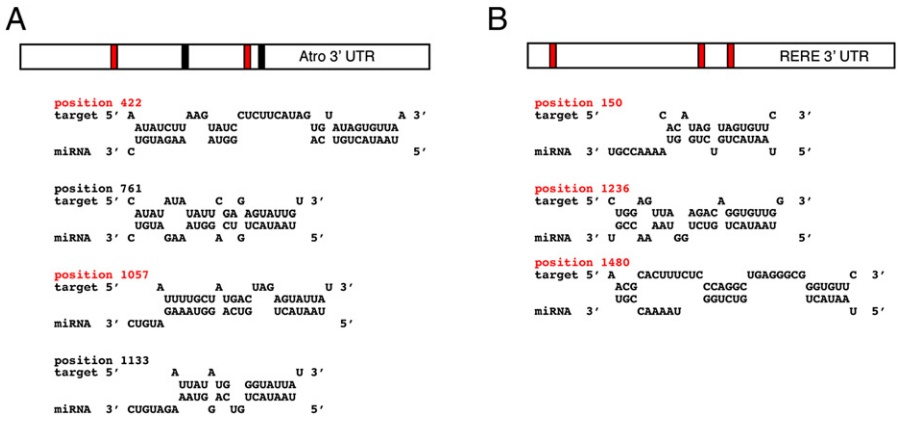

Figure 3. MiR-8 Target Sites Are Conserved

(A) Four potential miR-8 target sites in the *atrophin* 3′UTR. The sites depicted in red are conserved in *Drosophila pseudobscura*.

(B) Three potential target sites of miR-429, the 3′UTR of RERE. All are conserved in mouse.

prepared from brain, body wall (muscle and epidermis), and gut from wandering third instar larvae. Atrophin protein levels were detectably higher in *miR-8* mutant brain (Figure 5A) and in body wall but not in gut tissue (not shown). Two protein forms at ~280 kDa and a shorter ~150 kDa protein were expressed more strongly in the *miR-8* mutants than in the control animals. Although the predicted Mr of atrophin is ~260 kDa (Erkner et al., 2002), both of the ~280 kDa protein forms and the ~150 kDa protein were induced by Gal4-directed overexpression of the endogenous *atrophin* gene, confirming that they are authentic products of this locus.

If *atrophin* mRNA is a functionally important miR-8 target in vivo, we would expect that overexpression of atrophin protein contributes to the *miR-8* mutant phenotype. We therefore asked whether removing one copy of the *atrophin* gene would reduce the severity of the *miR-8* mutant phenotype. Reducing atrophin activity rescued the survival defect of the *mir-8* mutant by 50% (Figure 5B). The increase in survival was statistically significant (t test: 9.1×10^{-7}). The proportion of surviving adults that showed a leg defect was reduced by 40% (t test: 1.8×10^{-4}), and the leg malformations were less severe than in *miR-8* mutants with full atrophin activity. These observations suggest that misregulation of atrophin contributes to the defects observed in the *miR-8* mutant. To ask whether overproduction of atrophin is sufficient to cause these defects, we made use of a Gal4 *P* element insertion at the *miR-8* gene to direct overexpression of the endogenous *atrophin* gene in *miR-8*-expressing cells. These animals showed a similar spectrum of defects to the *miR-8* mutants. Survival was reduced, and the surviving animals

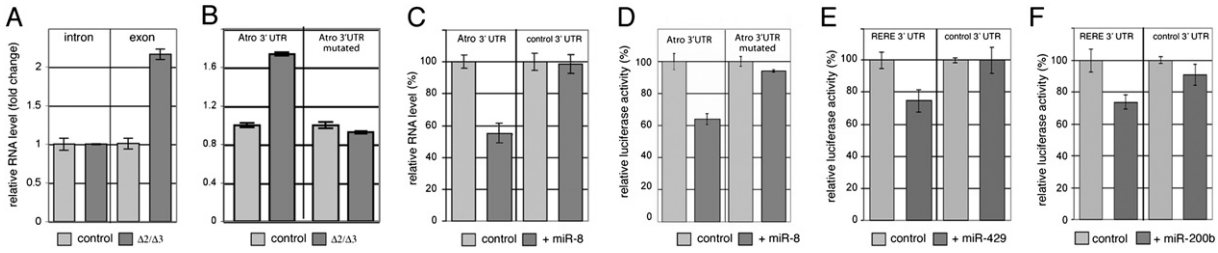

Figure 4. Posttranscriptional Regulation of *atrophin* RNA by MiR-8

(A) Real-time RT-PCR on *atrophin* using intron-specific primers (left) and exon-specific primers (right) in control and *miR-8* mutant animals (7 hr after puparium formation).

(B) Real-time RT-PCR on luciferase reporter transgenes containing either the normal *Drosophila atrophin* 3′UTR (left) or one where all four *miR-8*-binding sites were mutated in the seed sequence. Two or three nucleotides were exchanged per seed, such that consecutive binding between *miR-8* and the *atrophin* 3′UTR was interrupted at these positions. Transgenes were expressed under control of the tubulin promoter in control w^{1118} and *miR-8* mutant flies.

(C) Q-PCR on luciferase reporter transgenes containing either the normal *Drosophila atrophin* 3′UTR (left) or, as a control, the SV40 3′UTR (right). The 3′UTR luciferase reporter plasmids were coexpressed with miR-8 or a control.

(D) Normalized luciferase activity for a reporter transgene containing the *atrophin* 3′UTR and one where all four *miR-8*-binding sites were mutated. The 3′UTR was coexpressed with *miR-8* or with a vector-only control.

(E) Normalized luciferase activity for a reporter transgene containing the 3′UTR of RERE, the human *atrophin* ortholog, and a control 3′UTR. The 3′UTR was either coexpressed with miR-429, one of the human miR-8 orthologs, or a control.

(F) As (E), except for cotransfection with miR-200b. The data represents average ± SD for all panels.

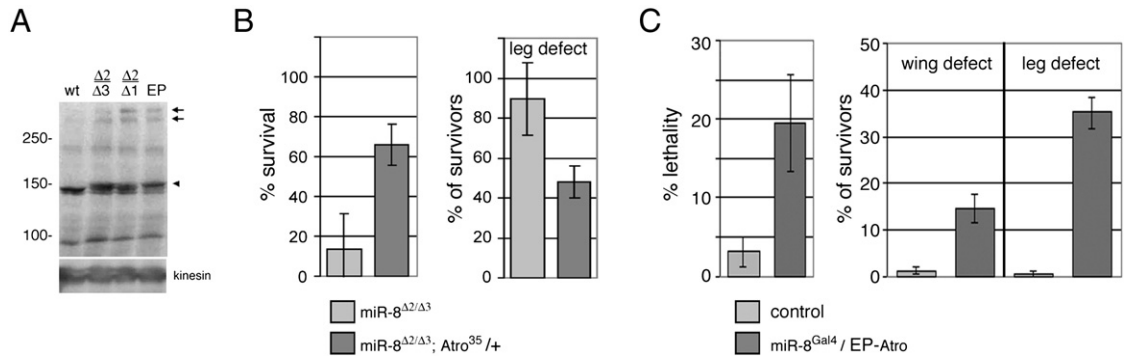

Figure 5. Atrophin Protein Levels Are Misregulated in *miR-8* Mutants and Contribute to Its Phenotypes

(A) Immunoblot showing atrophin protein levels in lysates prepared from third instar larval brains. Arrows indicate full-length atrophin protein forms at ~280 kDa. Arrowhead indicates a shorter form of atrophin protein (~150 kDa) that appears on Gal4-driven overexpression of the endogenous *atrophin* gene and in the *miR-8* mutants. Note: the band does not comigrate with the ~150 kDa band seen in the control sample (control: w^{1118} flies). EP: animals overexpressing atrophin under Gal4 control from an EP-element insertion at the endogenous *atrophin* gene. The origin of the various protein forms is unclear, particularly the shorter ~150 kDa form, as alternative RNA products that might account for these protein forms have not been reported.

(B) Histogram showing the effect of reducing *atrophin* activity in the *miR-8* mutant background. Removing one copy of *atrophin* in the $miR\text{-}8^{\Delta 2/\Delta 3}$ mutant rescued the survival defect by 50% (t test: 9.1×10^{-7}) and the leg defect by 40% (t test: 1.8×10^{-4}). The data represent an average ± SD for 13 batches of 100 flies for each genotype.

(C) Overexpressing *atrophin* under the control of $miR\text{-}8^{Gal4}$ results in phenotypes that strongly resemble the *miR-8* mutant ones. Survival and leg defects were similar to the ones of *miR-8*, and the wing phenotype was less penetrant. The data represent an average ± SD for 7 batches of 100 flies for each genotype.

showed leg and wing malformations resembling those in the *miR-8* mutants (Figure 5C).

Elevated Atrophin Levels Increase CNS Apoptosis and Cause Behavioral Defects in *miR-8* Mutants

The finding that misregulation of atrophin is responsible for at least part of the *miR-8* mutant phenotype is intriguing in light of the association of its mammalian orthologs, atrophin-1 and RERE with neurodegenerative disease and apoptosis (Kanazawa, 1999; Ross et al., 1999; Waerner et al., 2001). Bilen et al., (2006) have provided evidence that miRNAs, including the antiapoptotic miRNA *bantam* (Brennecke et al., 2003), limit the severity of polyglutamine repeat-induced neurodegeneration. In this context we asked whether the elevated expression of atrophin induced in *miR-8* mutants might be mediated through adverse effects on the nervous system. We observed an elevated level of apoptosis in the third instar larval brains of *miR-8* mutants, detected by antibody to the activated form of caspase 3 (Figure 6A). Expressing the endogenous atrophin gene in miR-8-expressing cells under miR-8 Gal4 control produced a comparable defect (Figure 6A), suggesting that elevated atrophin levels are largely responsible for the *miR-8* mutant defect. Although modest in magnitude at the third instar stage, in both cases these differences were statistically significant ($p < 0.05$). Comparison of miR-8 expression with caspase activation showed that a considerable fraction of the apoptotic cells in the brain were expressing miR-8 (compare Figures 6A and 6B). Increased expression of atrophin in these cells caused increased apoptosis.

The finding of elevated apoptosis in the brain raised the possibility of impaired central nervous system function. Impaired motor coordination could explain the eclosion defects observed in *miR-8* mutants. We next asked whether reducing apoptosis in the *miR-8* mutant could reduce the severity of the eclosion defect. In the course of these experiments, it became evident that low-level Gal4-independent expression of the transgene encoding the cell-death inhibitor p35 was sufficient to increase the number of *miR-8* mutant animals that eclosed successfully (Figure 6C). This difference was statistically significant ($p < 0.05$).

To further explore the possibility of impaired motor coordination in *miR-8* mutants, we made use of a simple behavioral assay. Flies are negatively geotactic, and normal animals climbed rapidly to the top of a tube (Figure 6D). For comparison with *miR-8* mutants, we selected only mutant flies that were morphologically normal and that had survived the early phase of posteclosion lethality. Such flies showed no reduction in lifespan compared to control flies, suggesting that they are not generally unhealthy (not shown). As such, they reflect the least impaired range of the mutant phenotypic spectrum. Yet, at 3 days of age, the *miR-8* mutants performed less well in the climbing assay. This difference was statistically significant ($p < 0.05$). A few mutant flies climbed as well as the controls, but most were slow, and many were unable to complete the task in the allotted time. The range of individual performance is reflected by the larger standard deviation for the *miR-8* mutants.

To ask whether the impaired performance in the climbing assay was due to elevated atrophin levels, we

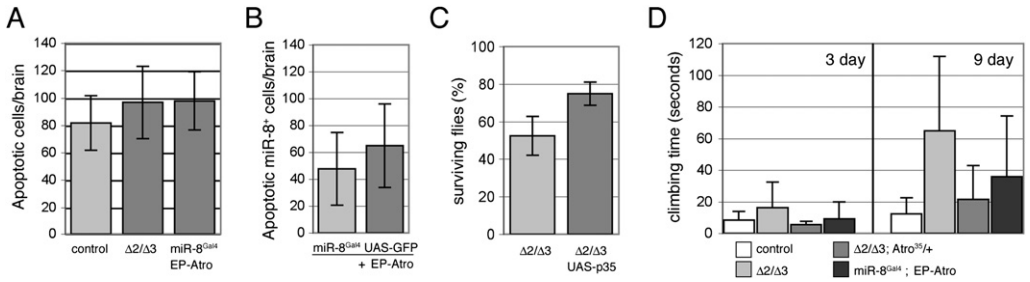

Figure 6. CNS Apoptosis and Behavioral Defects in *miR-8* Mutants

(A) Histogram showing the number of apoptotic cells in the brains of control and *miR-8* mutant third instar larvae. Apoptotic cells were detected by antibody to the activated form of caspase 3. Data represent the average (± SD). n = 32 for control, n = 27 for *miR-8*$^{\Delta 2/\Delta 3}$, and n = 16 for *miR-8*^{Gal4}*/EP-atro*.

(B) Histogram showing the number of apoptotic miR-8-expressing cells in the brains of third instar miR-8 Gal4 UAS-GFP larvae and larvae also expressing atrophin under miR-8 Gal4 control. miR-8-expressing cells were visualized by antibody to GFP. Apoptotic cells were detected by antibody to the activated form of caspase 3. Data represent the average (± SD). n = 21 for control (*miR-8*^{Gal4}*,UAS-GFP)* and n = 35 for *miR-8*^{Gal4}*,UAS-GFP/EP-atro*.

(C) Histogram showing survival of miR-8 mutants without and with a UAS-p35 transgene in the background. Leaky transcription of p35 partially rescued the survival defect of miR-8 mutants. The miR-8 mutant data represent an average ± SD for 5 batches and the data on miR-8 mutant plus UAS-p35 an average ± SD for 8 batches of 100 flies.

(D) Histogram showing the time needed for control, *miR-8* mutant (*miR-8*$^{\Delta 2/\Delta 3}$), *miR-8-atro* mutant (*miR-8*$^{\Delta 2/\Delta 3}$*;atro*^{35}) and *atro*-overexpressing (*miR-8*^{Gal4}*/EP-atro)* flies to climb to the top of a tube. The same flies were tested once 3 days and once 9 days posteclosion. Climbing ability reflects coordination. Data represent the average (± SD) for 30 flies (15 males and 15 females) of each genotype. Only morphologically normal mutants were used. Control flies climb rapidly to the top of a tube. Especially after 9 days, *miR-8* mutants climbed poorly and had not reached the top in 120 s, the maximum time allowed. However, some mutants performed as well as controls.

compared the performance of *miR-8* mutant flies with one or two copies of the *atrophin* gene. The performance of the flies with a lower level of atrophin activity was significantly improved at 3 days of age (Figure 6D; $p < 0.05$). At 9 days of age, *miR-8* mutants showed a greater impairment than in 3 day flies ($p < 0.001$), and this behavioral defect could still be ameliorated to a considerable degree by reduced *atrophin* expression ($p < 0.001$). By day 9, elevated atrophin expression in an otherwise normal fly under miR-8 Gal4 control was sufficient to cause a similar defect ($p < 0.05$). This defect was not yet apparent at day 3. Although the assay does not permit us to determine if the climbing defect is solely due to impaired motor coordination, it does suggest that elevated atrophin expression in the *miR-8* mutant causes a central nervous system disorder with behavioral consequences. The age dependence of this defect may reflect ongoing apoptosis in the central nervous system (CNS) due to persistent elevated atrophin expression. However, we do not exclude the possibility that a requirement for miR-8 function in other tissues might also contribute to these defects.

Atrophin Is a Tuning Target of MiR-8

Many miRNAs are thought to act by reducing expression of their targets to inconsequential levels, often by reducing target-RNA levels in the miRNA-expressing cells (Bartel and Chen, 2004; Lim et al., 2005; Farh et al., 2005; Stark et al., 2005; reviewed in Bushati and Cohen, 2007). It has also been suggested that miRNAs might, in some cases, buffer target levels, to prevent potentially detrimental excess expression while allowing required expression of the target. Bartel and Chen (2004) coined the term tuning targets to describe this relationship.

This mode of action implies a need for coexpression of the miRNA and its target. *atrophin* mRNA and protein have been reported to be ubiquitously expressed throughout development (Erkner et al., 2002; Zhang et al., 2002). miR-8 shows pattered expression in many tissues, including the CNS, where it overlaps with *atrophin* expression (Figure S3). In view of their coexpression and the observation that excess atrophin contributes to the *miR-8* phenotype, we wondered whether the regulatory relationship between miR-8 and *atrophin* might be of this type. To address this, we chose to selectively eliminate atrophin in miR-8-expressing cells by driving a UAS-atro$_{RNAi}$ transgene under control of miR-8 Gal4. Making use of the temperature sensitivity of Gal4 to increase expression of the RNAi construct, we found that at 29°C the survival rate of the atro$_{RNAi}$-expressing animals was reduced to about half of the level of the controls (Figure 7A). At 25°C the survival rate of the atro$_{RNAi}$-expressing animals decreased to ~70% the level of the controls but was further reduced to ~50% in atro$_{RNAi}$ flies lacking one copy of the endogenous *atrophin* gene, which reduces the starting level of *atrophin* expression (Figure 7B; $p < 0.05$). This enhancement of the severity of the RNAi phenotype is most consistent with an effect mediated by knocking down the endogenous *atrophin* gene rather than an off-target effect.

All surviving atro$_{RNAi}$-expressing animals showed extra wing veins, a phenotype previously described for clones of cells mutant for *atrophin* in the wing (Erkner et al., 2002; Zhang et al., 2002). This presumably reflects the effects of reduced *atrophin* expression in the miR-8-expressing cells in the wing imaginal disc (Figure S1F). The finding that reducing *atrophin* levels below the

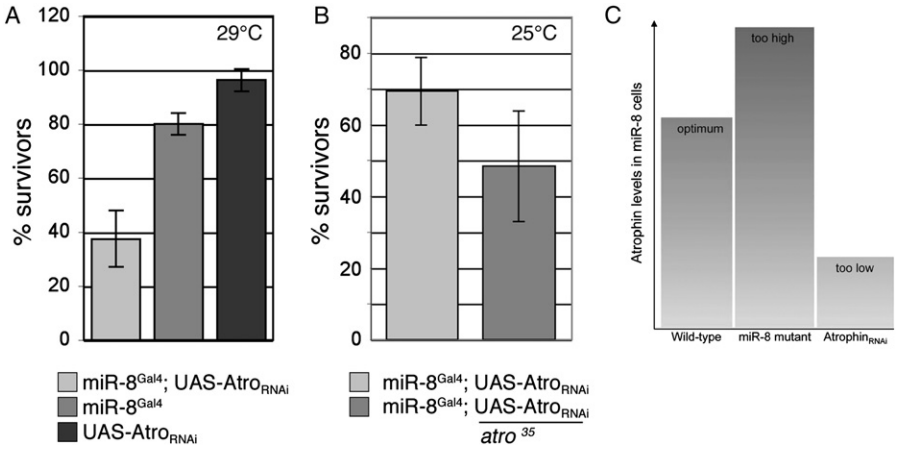

Figure 7. Atro Levels Are Tuned to Optimal Levels by *miR-8*

(A and B) Histograms showing survival of control and $atro_{RNAi}$-overexpressing flies. The UAS-$atro_{RNAi}$ transgene was expressed under control of miR-8^{GAL4} to knockdown atro expression in miR-8 cells. The data represent an average ± SD for four batches of 40 flies. In (A), flies were shifted to 29°C at the first instar larval stage. In (B), flies were raised at 25°C to reduce the effect of UAS-$atro_{RNAi}$ and permit comparison with flies mutant for one copy of *atro* (*atro*^{35}).

(C) We propose that *miR-8* functions to fine tune atro levels in order to guarantee its optimal concentrations in *miR-8*-expressing cells. Elevated atro levels, due to lack of *miR-8*, cause severe defects in animal survival, behavioral defects and increased apoptosis in the brain. Reduced atro levels lead to impaired survival indicating that residual levels of atro, after regulation through *miR-8*, have a function in *miR-8* cells.

threshold set by miR-8 causes defects that mirror known *atrophin* loss-of-function phenotypes suggests that miR-8-expressing cells require atrophin function (Figure 7C). Thus, *atrophin* can be considered to be a tuning target of miR-8.

DISCUSSION

Our findings suggest that misregulation of *atrophin* is an important factor contributing to the defects associated with loss of *miR-8* microRNA function. Atrophins are transcriptional corepressors, associated with histone deacetylase activity in *Drosophila* and in mammalian systems (Zhang et al., 2002; Zoltewicz et al., 2004; Wang et al., 2006). Elevated expression of a transcriptional corepressor could be responsible for the extensive transcriptional changes observed in *miR-8* mutants. Indeed, misregulation of transcription is thought to be a major cause of the neurodegeneration associated with trinucleotide repeat-expansion diseases, such as dentatorubral-pallidoluysian atrophy (DRPLA), which is caused by atrophin-1 (reviewed in Riley and Orr, 2006). RERE is the more similar of the two mammalian atrophins to *Drosophila* atrophin. RERE shares regulation by the miR-8-related miRNAs, miR-200b and miR-429, as well as the ability to recruit HDACs and serve as a transcriptional corepressor. In this context, it is of particular interest that HDAC inhibitors have been found to be effective against trinucleotide repeat-expansion cytotoxicity (Kariya et al., 2006).

Vertebrates have multiple miR-8-related miRNAs: there are two in mammals and four in zebrafish. In zebrafish, two *miR-8* family members are expressed in a subset of peripheral sensory organs, known as the lateral line (Wienholds et al., 2005). Overexpression of *miR-200a* or *miR-200b* results in impaired migration of the sense organ primordia and therefore fewer sense organs along the lateral line (Ason et al., 2006). One of the phenotypes observed in *RERE* mutant zebrafish is a reduced number of lateral-line sense organs (Asai et al., 2006). The resemblance between the consequences of overexpressing the *miR-8* family members *miR-200a* and *miR-200b* and the *RERE* mutant phenotype is striking. It is therefore tempting to speculate that the regulatory relationship between *atrophin* and miR-8 might be conserved in zebrafish.

miRNAs have been implicated in neurodegeneration caused by a polygutamine repeat-expansion disease model in *Drosophila* (Bilen et al., 2006). Loss of all miRNAs, using mutants that remove proteins required for miRNA biogenesis, caused increased sensitivity to polygutamine repeat-induced neurodegeneration. Our findings suggest that elevated expression of atrophin, resulting from loss of *miR-8*, is sufficient to cause CNS apoptosis and to impair performance in a behavioral assay. Although the climbing assay may seem deceptively simple, to perform it the fly must be able to determine which way is up, sense the position of its limbs, and coordinate its movements. Each of these depends on complex neural functions, and the flies' ability to perform them might be impaired as a consequence of the elevated CNS apoptosis. It is worth noting that reducing apoptosis suppressed the pupal eclosion defect of the *miR-8* mutants, which may also have a motor coordination basis. It is tempting to interpret the age dependence of the impaired performance of *miR-8* mutants in the climbing assay as a sign of progressive neurodegeneration resulting from to persistently elevated atrophin levels. We note that the effects in the

mutant are likely concentrated in miR-8-expressing neurons and, so, do not affect all neural functions. Indeed, the mutant flies that survive beyond the first day after eclosion do not show the reduced lifespan associated with massive general neurodegeneration (e.g., Bilen et al., 2006). The ability of mammalian miR-200b and miR-429 to downregulate RERE raises the possibility that they might limit HDAC activity. If so, mutations in miR-200b and miR-429 might be worth exploring as potential risk factors for DRPLA.

Recent computational and experimental studies have suggested that many miRNAs show essentially reciprocal patterns of expression to their target RNAs, with target RNA levels being naturally low in the miRNA-expressing cells or tissues (Lim et al., 2005; Stark et al., 2005; Farh et al., 2005). This has led to the proposal that the main role of many miRNAs is to reduce target-RNA expression to inconsequential levels. Bartel & Chen (2004) also proposed that some miRNA-target relationships may be described as tuning, in which the miRNA buffers target expression levels. A critical distinction between the switch and tuning modes of regulation is that in switch mode the target is reduced to an inconsequential level, whereas in the tuning mode the remaining level of target expression must be required in the miRNA-expressing cell (reviewed in Bushati and Cohen, 2007). We have provided evidence that the relationship between miR-8 and atrophin constitutes an example of the latter type. Both atrophin and miR-8 are very broadly expressed during development, and our findings indicate that further reducing the expression of atrophin in miR-8-expressing cells causes developmental defects. Thus, the level of atrophin resulting from miR-8-mediated regulation can be seen as being optimal for these cells—neither too high nor too low (illustrated in Figure 7C).

EXPERIMENTAL PROCEDURES

Fly Strains

mir-8^{Gal4} (P{GawB}NP5247) was obtained from the Kyoto stock center. P{EP}2269 and P{EP}2239 were obtained from the Szeged stock center. The *Drosophila atrophin* gene is also known as *grunge* (Erkner et al., 2002). EP-atro, P{EPgy2}^{GugEY14339}, used for atrophin overexpression, and the P(LacZ w^{+})*gug*^{j5A3} (atro-lacZ) line were obtained from the Bloomington stock center, and are described in flybase (http://flybase.bio.indiana.edu). UAS-atro$_{RNAi}$ flies were obtained from Barry Dixon.

Mutant Generation

Targeted homologous recombination was performed as described (Gong and Golic, 2003). Left and right arms of the targeting vector were prepared by PCR of 3 kb fragments from BAC DNA using oligos GCAgcggccgcGGCATGGGATTGGACTTGG and ATGgcatgcCTAATTAGCAAGATTCGGTATTC for the left flank and GTCggcgcgccAGAGTGGATAATGCGAAGACAAG and TAAcgtacgCGGAAAGTCATAGAAAGCGATAG for the right flank. Transgenic flies carrying the targeting construct were crossed to flies with heat-inducible *FLP* recombinase and *I-SceI* endonuclease (*70FLP* and *70I-SceI*, Bloomington Stock Center), and the resulting progeny were heat shocked for 45 min at 38°C on day 3 of development. Mosaic-eyed females were crossed to If/CyO males. Targeting events were mapped to the second chromosome in the next generation. Imprecise excisions were generated by crossing P{EP}2239 and P{EP}2269 to flies expressing the Δ2-3 transposase (Robertson et al., 1988). Deletions in the excisions *miR-8*$^{\Delta 1}$ and *miR-8*$^{\Delta 2}$ were determined by sequencing DNA fragments spanning the breakpoints.

Northern Blots

Total RNA from adult flies was resolved on a 15% denaturing acrylamide gel. Fifteen micrograms of RNA were loaded per lane. As a control *w*^{1118} flies were used. The blot was probed with a 23 nt 5′ end-labeled oligonucleotide complementary to the mature form of miR-8 (GAC ATCTTTACCTGACAGTATTA), end-labeled with T4 polynucleotide kinase (New England Biolabs). A tRNA probe was used as a loading control (Lagos-Quintana et al., 2001).

miRNA-3′UTR Alignment

microRNA-3′UTR alignment was performed using the BiBiServ server (Rehmsmeier et al., 2004; http://bibiserv.techfak.uni-bielefeld.de/rnahybrid/submission.html).

Microarray

Probe preparation and hybridization were as described in Sandmann et al., (2006). The microarrays contained clones from the *Drosophila* DGC1 and DGC2 collections. To identify genes differentially expressed *miR-8* mutant pupae were compared with stage-matched controls. A one-class Significance Analysis of Microarrays (Tusher et al., 2001) was performed on two different mutant combinations, *miR-8*$^{\Delta 2/\Delta 1}$ or *miR-8*$^{\Delta 2/\Delta 3}$, compared to *w*^{1118} controls. Genes with significance score of $q < 0.05$ and a fold enrichment of $\log2 > 0.7$ or < -0.7 were considered to be differentially regulated.

Quantitative RT-PCR

PCRs were performed using the ABI7500 machine and the ABI SYBR green system. Measurements were normalized to mitochondrial large ribosomal RNA (mtlrRNA1, 5′-AAAAAGATTGCGACCTCGAT and 5′-AAACCAACCTGGCTTACACC). Nuclear, intron-containing RNA is not subject to miRNA posttranscriptional regulation. We therefore performed Q-PCR on an intron versus an exon to assay transcription levels of the *atrophin* locus, as distinct from mRNA levels. Primers to assay intron containing RNA are 5′-GCCTTGCTTATCTTCGAAACC and 5′-TCCAGCCTTTTAATGCGTCT. Primers to assay mRNA levels are 5′-CCATCCGACGGAGCCATTGCCC and 5′-CATTCGGTGTCGTCCGGTTTTG. Firefly luciferase primers are 5′-CCGCCGTTGTTGTTTTG and 5′-CTCCGCGCAACTTTTTC Renilla luciferase primers are 5′-CGGACCCAGGATTCTTTT and 5′-TTGCGAAAAATGAAGACCT.

UTR Reporter Assays

Luciferase 3′UTR reporter and miRNA plasmids were expressed under control of the tubulin promoter. miR-8 was expressed from a plasmid containing a 400 bp genomic region, including the hairpin. S2 cells were transfected in 24-well plates with 0.025 μg of the firefly luciferase reporter plasmid, 0.025 μg of a *Renilla* luciferase expressing plasmid (transfection control), and 0.25 μg of the miRNA expression plasmid or empty vector. Transfections were performed in triplicate. Dual-luciferase assays (Promega) were performed 2.5 days after transfection according to the manufacturer's protocol.

Immunoblotting

Protein lysates were prepared from late third instar larval brains by crushing them in SDS sample-loading buffer and boiling the samples for 5 min. Samples were loaded onto 6% SDS-PAGE gels and transferred to a nitrocellulose membrane via wet transfer overnight at 150 mA. The nitrocellulose membrane was incubated with specific antibodies diluted in 5% fat-free milk. The rabbit anti-atrophin (D3) (Erkner et al., 2002) was used at a 1:1000 dilution. The protein bands were visualized using anti-rabbit secondary antibody conjugated with HRP (used 1:5000) followed by ECL Chemiluminiscence reagent according

to the manufacturer's instructions (Perkin-Elmer). Membranes were stripped and reprobed with rabbit anti-Kinesin (Cytoskeleton) used at a 1:10,000 dilution.

miRNA In Situs

Pri-miRNA transcript in situ hybridization was as described (Kosman et al., 2004) except for the following: embryos were not treated with Xylene, anti-pri-miRNA probes were labeled with DIG-11 UTP but not hydrolyzed, and probes were detected with primary anti-DIG POD antibody (1:200; Roche #1207733). miRNA was detected first with the tyramide signal-amplification method (Molecular Probes #T-20939; 2 hr at room temperature). To obtain a better signal, a second amplification round was performed using HRP coupled anti-oregon green antibody (1:400; Molecular Probes #A21253).

Immunocytochemistry

Embryos and imaginal discs were fixed in 4% formaldehyde and stained with standard methods. Embryos were stained with mouse anti-engrailed (used 1:10), rabbit anti-dMef-2 (1:250), and mouse and rabbit anti-GFP (used 1:200). Imaginal discs were stained with mouse anti-GFP. For detecting apoptotic cells, late third instar larval brains were stained with rabbit anti-cleaved caspase 3 (Asp175) (Cell Signaling Technology, used 1:200). Primary antibodies were incubated overnight at 4°C and secondary antibody for 3 hr at room temperature.

Quantitative Measurement of the Occurrence of Apoptosis

To count the number of apoptosis-positive spots in the images, we developed the following image analysis protocol using ImageJ version 1.38a (WS Rasband, NIH, Bethesda, Maryland, USA; http://rsb.info.nih.gov/ij/). Three-dimensional 8-bit image data were converted to two-dimensional images by maximum intensity projection along the Z axis onto the XY plane. A duplicate of this projection image was created, and a Gaussian filter with 20 px diameter was applied to blur the duplicate to prepare the background image. The original projection image was subtracted from the blurred duplicate to obtain a background-subtracted image. This subtracted image was threshold filtered (minimum threshold level at 12 and maximum at 255). The binary image still contains noise from the acquisition. To remove this noise, the open operation was applied. Finally, we measured the number of particles within the processed image automatically while leaving out particles larger than 12 px that are expected to be due to nonspecific labeling. The ImageJ macro used for this automatic measurement is available on request.

Colocalization of *miR-8* Positive and Apoptotic Cells

miR-8 Gal4, UAS-GFP allowed us to count apoptosis via anti-caspase 3 staining in *miR-8*-expressing cells. To measure the degree of colocalization of *miR-8* expression and apoptosis, we threshold filtered stacks from each channel and binarized the images. To segment the signal successfully, various threshold values were tested manually, and sufficient threshold values were determined for each channel prior to image processing. We then counted the number of apoptosis channel pixels overlapping with the GFP channel signal. The measurement was done for each Z slice, and then the values were summed for the 3D data set from each brain. A macro was written for the semiautomation of these measurements using an image processing/analysis software ImageJ (Rasband, W.S., U. S. National Institutes of Health, Bethesda, Maryland, USA; http://rsb.info.nih.gov/ij/).

Climbing Assay

Single flies were placed in an empty vial, marked with a line 5 cm from the bottom. Flies were allowed to rest for 15 min before being tapped down to the bottom of the vial. The time required to climb and cross the 5 cm line was recorded with a cutoff at 120 s. Thirty flies (fifteen males and fifteen females) of each genotype were scored. Flies were raised in comparable uncrowded conditions at 25°C. The same flies were tested once at 3 days and again at 9 days posteclosion.

Supplemental Data

Supplemental Data include three figures, one table, and a movie and can be found with this article online at http://www.cell.com/cgi/content/full/131/1/136/DC1/.

ACKNOWLEDGMENTS

We thank Steve Kerridge and Eileen Furlong for reagents; Jan Huisken for help with the movie; Kota Miura for help with image analysis; Bernard Charroux, Helen McNeill, and Kent Duncan for helpful discussions; and Ann-Marie Voie and Eva Loeser for technical help.

Received: November 8, 2006
Revised: August 22, 2007
Accepted: September 14, 2007
Published: October 4, 2007

REFERENCES

Asai, Y., Chan, D.K., Starr, C.J., Kappler, J.A., Kollmar, R., and Hudspeth, A.J. (2006). Mutation of the atrophin2 gene in the zebrafish disrupts signaling by fibroblast growth factor during development of the inner ear. Proc. Natl. Acad. Sci. USA *103*, 9069–9074.

Ason, B., Darnell, D.K., Wittbrodt, B., Berezikov, E., Kloosterman, W.P., Wittbrodt, J., Antin, P.B., and Plasterk, R.H. (2006). Differences in vertebrate microRNA expression. Proc. Natl. Acad. Sci. USA *103*, 14385–14389.

Bartel, D.P., and Chen, C.Z. (2004). Micromanagers of gene expression: the potentially widespread influence of metazoan microRNAs. Nat. Rev. Genet. *5*, 396–400.

Behm-Ansmant, I., Rehwinkel, J., and Izaurralde, E. (2006). MicroRNAs silence gene expression by repressing protein expression and/or by promoting mRNA decay. Cold Spring Harb. Symp. Quant. Biol. *71*, 523–530.

Bilen, J., Liu, N., Burnett, B.G., Pittman, R.N., and Bonini, N.M. (2006). MicroRNA pathways modulate polyglutamine-induced neurodegeneration. Mol. Cell *24*, 157–163.

Brennecke, J., Hipfner, D.R., Stark, A., Russell, R.B., and Cohen, S.M. (2003). *bantam* encodes a developmentally regulated microRNA that controls cell proliferation and regulates the pro-apoptotic gene hid in Drosophila. Cell *113*, 25–36.

Brennecke, J., Stark, A., Russell, R.B., and Cohen, S.M. (2005). Principles of microRNA-target recognition. PLoS Biol. *3*, e85.

Bushati, N., and Cohen, S.M. (2007). microRNA functions. Annu. Rev. Cell Dev. Biol. *23*, 175–205.

Erkner, A., Roure, A., Charroux, B., Delaage, M., Holway, N., Core, N., Vola, C., Angelats, C., Pages, F., Fasano, L., and Kerridge, S. (2002). Grunge, related to human Atrophin-like proteins, has multiple functions in Drosophila development. Development *129*, 1119–1129.

Farh, K.K., Grimson, A., Jan, C., Lewis, B.P., Johnston, W.K., Lim, L.P., Burge, C.B., and Bartel, D.P. (2005). The widespread impact of mammalian microRNAs on mRNA repression and evolution. Science *310*, 1817–1821.

Fortier, T.M., Vasa, P.P., and Woodard, C.T. (2003). Orphan nuclear receptor betaFTZ-F1 is required for muscle-driven morphogenetic events at the prepupal-pupal transition in Drosophila melanogaster. Dev. Biol. *257*, 153–165.

Fristrom, D., and Fristrom, J. (1993). The metamorphic development of the adult epidermis. In Drosophila Development, A. Martinez Arias and M. Bate, eds. (Cold Spring Harbor: Cold Spring Harbor Press), pp. 843–897.

Giraldez, A.J., Cinalli, R.M., Glasner, M.E., Enright, A.J., Thomson, J.M., Baskerville, S., Hammond, S.M., Bartel, D.P., and Schier, A.F.

(2005). MicroRNAs regulate brain morphogenesis in zebrafish. Science *308*, 833–838.

Giraldez, A.J., Mishima, Y., Rihel, J., Grocock, R.J., Van Dongen, S., Inoue, K., Enright, A.J., and Schier, A.F. (2006). Zebrafish miR-430 promotes deadenylation and clearance of maternal mRNAs. Science *312*, 75–79.

Gong, W.J., and Golic, K.G. (2003). Ends-out, or replacement, gene targeting in Drosophila. Proc. Natl. Acad. Sci. USA *100*, 2556–2561.

Grun, D., Wang, Y.L., Langenberger, D., Gunsalus, K.C., and Rajewsky, N. (2005). microRNA target predictions across seven Drosophila species and comparison to mammalian targets. PLoS Comput. Biol *1*, e13.

Hornstein, E., and Shomron, N. (2006). Canalization of development by microRNAs. Nat. Genet. *38* (*Suppl.*), S20–S24.

Kanazawa, I. (1999). Molecular pathology of dentatorubral-pallidoluysian atrophy. Philos. Trans. R. Soc. Lond. B Biol. Sci. *354*, 1069–1074.

Kariya, S., Hirano, M., Uesato, S., Nagai, Y., Nagaoka, Y., Furiya, Y., Asai, H., Fujikake, N., Toda, T., and Ueno, S. (2006). Cytoprotective effect of novel histone deacetylase inhibitors against polyglutamine toxicity. Neurosci. Lett. *392*, 213–215.

Kloosterman, W.P., and Plasterk, R.H. (2006). The diverse functions of microRNAs in animal development and disease. Dev. Cell *11*, 441–450.

Kosman, D., Mizutani, C.M., Lemons, D., Cox, W.G., McGinnis, W., and Bier, E. (2004). Multiplex detection of RNA expression in Drosophila embryos. Science *305*, 846.

Krek, A., Grun, D., Poy, M.N., Wolf, R., Rosenberg, L., Epstein, E.J., MacMenamin, P., da Piedade, I., Gunsalus, K.C., Stoffel, M., and Rajewsky, N. (2005). Combinatorial microRNA target predictions. Nat. Genet. *37*, 495–500.

Lagos-Quintana, M., Rauhut, R., Lendeckel, W., and Tuschl, T. (2001). Identification of novel genes coding for small expressed RNAs. Science *294*, 853–858.

Lewis, B.P., Burge, C.B., and Bartel, D.P. (2005). Conserved seed pairing, often flanked by adenosines, indicates that thousands of human genes are microRNA targets. Cell *120*, 15–20.

Li, Y., Wang, F., Lee, J.A., and Gao, F.B. (2006). MicroRNA-9a ensures the precise specification of sensory organ precursors in Drosophila. Genes Dev. *20*, 2793–2805.

Lim, L.P., Lau, N.C., Garrett-Engele, P., Grimson, A., Schelter, J.M., Castle, J., Bartel, D.P., Linsley, P.S., and Johnson, J.M. (2005). Microarray analysis shows that some microRNAs downregulate large numbers of target mRNAs. Nature *433*, 769–773.

Mallory, A.C., and Vaucheret, H. (2006). Functions of microRNAs and related small RNAs in plants. Nat. Genet. Suppl. *38*, S31–S36.

Nolo, R., Abbott, L.A., and Bellen, H.J. (2000). Senseless, a Zn finger transcription factor, is necessary and sufficient for sensory organ development in Drosophila. Cell *102*, 349–362.

Rehmsmeier, M., Steffen, P., Hochsmann, M., and Giegerich, R. (2004). Fast and effective prediction of microRNA/target duplexes. RNA *10*, 1507–1517.

Rehwinkel, J., Natalin, P., Stark, A., Brennecke, J., Cohen, S.M., and Izaurralde, E. (2006). Genome-wide analysis of mRNAs regulated by Drosha and Argonaute proteins in Drosophila melanogaster. Mol. Cell. Biol. *26*, 2965–2975.

Riley, B.E., and Orr, H.T. (2006). Polyglutamine neurodegenerative diseases and regulation of transcription: assembling the puzzle. Genes Dev. *20*, 2183–2192.

Robertson, H.M., Preston, C.R., Phillis, R.W., Johnson-Schlitz, D.M., Benz, W.K., and Engels, W.R. (1988). A stable genomic source of P element transposase in Drosophila melanogaster. Genetics *118*, 461–470.

Ross, C.A., Wood, J.D., Schilling, G., Peters, M.F., Nucifora, F.C., Jr., Cooper, J.K., Sharp, A.H., Margolis, R.L., and Borchelt, D.R. (1999). Polyglutamine pathogenesis. Philos. Trans. R. Soc. Lond. B Biol. Sci. *354*, 1005–1011.

Sandmann, T., Jensen, L.J., Jakobsen, J.S., Karzynski, M.M., Eichenlaub, M.P., Bork, P., and Furlong, E.E. (2006). A temporal map of transcription factor activity: mef2 directly regulates target genes at all stages of muscle development. Dev. Cell *10*, 797–807.

Stark, A., Brennecke, J., Bushati, N., Russell, R.B., and Cohen, S.M. (2005). Animal MicroRNAs confer robustness to gene expression and have a significant impact on 3′UTR evolution. Cell *123*, 1133–1146.

Teleman, A.A., Maitra, S., and Cohen, S.M. (2006). Drosophila lacking microRNA miR-278 are defective in energy homeostasis. Genes Dev. *20*, 417–422.

Tusher, V.G., Tibshirani, R., and Chu, G. (2001). Significance analysis of microarrays applied to the ionizing radiation response. Proc. Natl. Acad. Sci. USA *98*, 5116–5121.

Waerner, T., Gardellin, P., Pfizenmaier, K., Weith, A., and Kraut, N. (2001). Human RERE is localized to nuclear promyelocytic leukemia oncogenic domains and enhances apoptosis. Cell Growth Differ. *12*, 201–210.

Wang, L., Rajan, H., Pitman, J.L., McKeown, M., and Tsai, C.C. (2006). Histone deacetylase-associating Atrophin proteins are nuclear receptor corepressors. Genes Dev. *20*, 525–530.

Wienholds, E., Kloosterman, W.P., Miska, E., Alvarez-Saavedra, E., Berezikov, E., de Bruijn, E., Horvitz, R.H., Kauppinen, S., and Plasterk, R.H. (2005). MicroRNA Expression in Zebrafish Embryonic Development. Science *309*, 310–311.

Xie, X., Lu, J., Kulbokas, E.J., Golub, T.R., Mootha, V., Lindblad-Toh, K., Lander, E.S., and Kellis, M. (2005). Systematic discovery of regulatory motifs in human promoters and 3′ UTRs by comparison of several mammals. Nature *434*, 338–345.

Zhang, S., Xu, L., Lee, J., and Xu, T. (2002). Drosophila atrophin homolog functions as a transcriptional corepressor in multiple developmental processes. Cell *108*, 45–56.

Zoltewicz, J.S., Stewart, N.J., Leung, R., and Peterson, A.S. (2004). Atrophin 2 recruits histone deacetylase and is required for the function of multiple signaling centers during mouse embryogenesis. Development *131*, 3–14.

Accession Numbers

The microarray data have been deposited in Array Express at the EBI under accession number E-TABM-33.